Respiratory Physiology & Neurobiology 208 (2015) 45–50

Contents lists available at ScienceDirect

Respiratory Physiology & Neurobiology

journal homepage: www.elsevier.com/locate/resphysiol

Developmental nicotine exposure adversely effects respiratory patterning in the barbiturate anesthetized neonatal rat

Santiago Barreda, Ian J. Kidder, Jordan A. Mudery, E. Fiona Bailey*

Department of Physiology, College of Medicine, University of Arizona, Tucson, AZ 85721-0093, USA

ARTICLE INFO

Article history:
Accepted 7 January 2015
Available online 14 January 2015

Keywords:
Nicotine
Sudden infant death syndrome
Autocorrelation function

ABSTRACT

Neonates at risk for sudden infant death syndrome (SIDS) are hospitalized for cardiorespiratory monitoring however, monitoring is costly and generates large quantities of averaged data that serve as poor predictors of infant risk. In this study we used a traditional autocorrelation function (ACF) testing its suitability as a tool to detect subtle alterations in respiratory patterning in vivo. We applied the ACF to chest wall motion tracings obtained from rat pups in the period corresponding to the mid-to-end of the third trimester of human pregnancy. Pups were drawn from two groups: nicotine-exposed and saline-exposed at each age (i.e., P7, P8, P9, and P10). Respiratory-related motions of the chest wall were recorded in room air and in response to an arousal stimulus (F_IO_2 14%). The autocorrelation function was used to determine measures of breathing rate and respiratory patterning. Unlike alternative tools such as Poincare plots that depict an *averaged* difference in a measure breath to breath, the ACF when applied to a digitized chest wall trace yields an *instantaneous* sample of data points that can be used to compare (data) points at the same time in the next breath or in any subsequent number of breaths. The moment-to-moment evaluation of chest wall motion detected subtle differences in respiratory pattern in rat pups exposed to nicotine in utero and aged matched saline-exposed peers. The ACF can be applied online as well as to existing data sets and requires comparatively short sampling windows (~2 min). As shown here, the ACF could be used to identify factors that precipitate or minimize instability and thus, offers a quantitative measure of risk in vulnerable populations.

1. Introduction

Sudden infant death syndrome (SIDS) is defined as the sudden sleep related death of an infant <12 months of age that is unexplained despite an autopsy and post-mortem examination (Hilaire et al., 2010; Willinger et al., 1991). Maternal tobacco smoking or exposure to environmental tobacco smoke are major risk factors for SIDS (Mitchell and Milerad, 2006) and infants born to mothers that smoke exhibit increased nicotinic acetylcholine receptor expression in brainstem nuclei that control normal respiration, arousal (Cohen et al., 2005; Duncan et al., 2008; Machaalani et al., 2011) and integrate information from cardiovascular, pulmonary, respiratory tract and gastrointestinal receptor afferents (Machaalani et al., 2011; Machaalani and Waters, 2008; Waters et al., 1999). Despite neuro-pathologic evidence of morphological and receptor binding abnormalities affecting multiple brainstem nuclei (Jaiswal et al., 2013; Machaalani et al., 2011; Slotkin et al., 1987; Smith et al., 2010), there is no consistent phenotype associated with gestational or developmental exposure to cigarette smoke or to nicotine. And, although SIDS victims show a higher incidence of respiratory abnormalities including apneas, delayed arousal responses and diminished ventilatory chemo-reflexes, the frequency of those events is low and of limited diagnostic and therapeutic utility.

There is a pressing need for novel approaches to better identify respiratory patterns that may increase the risk for SIDS. One approach to the problem has been the use of nonlinear analyses such as Poincaré plots (Barrett et al., 2012; Brennan et al., 2002; Dick et al., 2014). Although this approach also can be used to detect respiratory instability, Poincare plots represent an average of the data points within the breath rather than considering individual data points within each breath. In view of this limitation, we applied a standard autocorrelation function (ACF) to digitized respiration-related chest wall motion traces to obtain *unrestricted* estimates of respiratory system stability using this approach to test the hypothesis that rats exposed to nicotine in utero i.e., subject to developmental nicotine exposure (DNE), will exhibit greater respiratory instability relative to age-matched, sham-treated controls.

* Corresponding author. Tel.: +1 520 6268299.
E-mail address: ebailey@arizona.edu (E.F. Bailey).

http://dx.doi.org/10.1016/j.resp.2015.01.005
1569-9048/

2. Materials and methods

2.1. Study animals

Thirty-four Sprague-Dawley rat pups (Charles-River Laboratories) were studied on postnatal days 7–10 (P7–P10). Pups were drawn from two experimental groups: nicotine-exposed ($n = 11$) and saline-exposed ($n = 23$) at each age (i.e. P7, P8, P9, and P10) corresponding to the developmental stage of preterm and term human infants (i.e., mid-to-end of the third trimester of human pregnancy) (Clancy et al., 2007). Animals had access to nutrition via the dam and were housed under a 12 h light/12 h dark cycle. All experimental procedures were approved by the Institutional Animal Care and Use Committee at the University of Arizona and adhered to the Public Health Service Policy on Humane Care and Use of Laboratory Animals.

2.2. Developmental nicotine and saline exposure

Procedures related to nicotine and saline exposure were based on prior reports (Luo et al., 2004; Robinson et al., 2002). Briefly, pregnant dams were delivered to the Animal Care facility at the University of Arizona and given 24 h to acclimate. On the following day, dams were anesthetized via intramuscular injection of 0.75 cc kg^{-1} "rabbit mix" (5 cc ketamine, 8 cc 20 mg ml^{-1} xylazine, 2 cc acepromazine) into the hind limb, followed by a subcutaneous injection of analgesic (Buprenex, 0.5 mg kg^{-1}) and preparation of the surgical site. Absence of limb withdrawal to paw pressure was assessed every 15 min to confirm a sufficient plane of anesthesia.

An incision was made at the base of the neck and an osmotic mini pump (Alzet 2ML4, Durect Corp., Cupertino, CA) was inserted through the incision and sutured shut (nylon). Antibiotics (Combi-Pen-48, Bimedi Inc.) were provided via a subcutaneous injection upon completion of the surgery. Post-operative care included analgesia (Buprenex, 0.5 mg kg^{-1}) every 12 h for a period of 36 h and an antibiotic injection 24 h post-surgery. Surgeries were performed on embryonic day 5 to coincide with embryonic implantation in the uterine wall (Serra et al., 2001) and pumps were charged to deliver saline or nicotine bitartrate at 6 mg kg^{-1} day^{-1} which corresponds to 2.1 mg kg^{-1} day^{-1} of free base nicotine; similar to a moderate to heavy smoker (Stephan-Blanchard et al., 2013). Because the Alzet 2ML4 pump delivers over 28 days, pups were exposed to nicotine or saline through the remainder of gestation to P10 via milk from the dam hence, we use the term developmental nicotine exposure (DNE) to indicate exposure to nicotine that continues after birth.

2.3. Study design

The following experimental conditions applied to *all* pups. Pups were studied in a flow through chamber the details of which have been published elsewhere (Kidder et al., 2014). Pups were sedated via an intraperitoneal injection of barbiturate (35 mg kg^{-1}, Inactin hydrate, Sigma–Aldrich) to minimize movement and to permit recording of respiratory-related motions of the chest wall. Sedation was titrated on the basis of breathing rate and did not drop below 110 ± 10 breaths min^{-1}. Chest wall motions were detected via a force transducer (World Precision Instruments, FORT100) in contact with the chest wall. Pups' respiration was recorded for 2 min in room air and in normocapnic hypoxia (0.14 F_IO_2) to assess the arousal response. Humidified gas mixtures were introduced into the chamber via a rotameter (Matheson Tri-gas, model FM-1050-VO-3T). The composition of the inspired gas was mixed online and monitored with O_2 and CO_2 gas analyzers (VacuMed 17518 and 17515). Rectal temperature was obtained via a thermocouple probe (IT-18, Physitemp Instruments) and maintained at 37 ± 0.9 °C with a heating pad. Temperature and humidity were controlled online and monitored via a thermometer hygrometer (FLUKER'S CF-22642). Experimental sessions were captured on video using a Microsoft LifeCam Studio web camera synchronized with EMG signals via Spike2 (version 7.1) software. All data were recorded using Spike2 software (Cambridge Electronic Design, UK) and analyzed off-line in MATLAB. For each pup, we obtained 2 min of chest wall motion associated with an otherwise stable period of rest breathing uninterrupted by movement or apnea was included in the analysis (see Fig. 1).

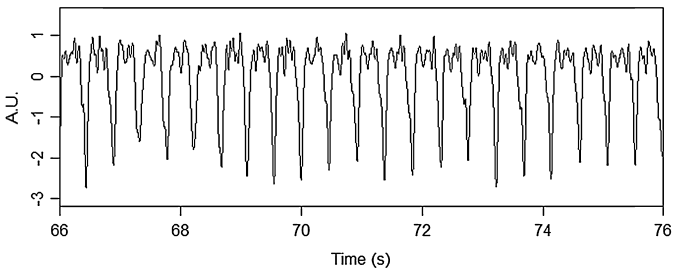

Fig. 1. Representative chest wall motion traces from a saline exposed pup obtained on post-natal day 7. Negative deflections correspond to inspirations (i.e., chest wall expansion). Note periodic oscillations in the magnitude of the chest wall excursion.

Breathing rates were measured by summation of peak chest wall expansions (inspirations) in 1-min epochs for each gas condition. Heart rates were determined from the EKG signal obtained from the intercostal EMG lead and R wave events were discriminated from the lead signal and summed over 1-min epochs for each gas condition. Initially, we used a univariate ANOVA to assess differences in body mass between DNE and saline pups and assessed the effects of experimental group and post-natal age on average heart rate and breathing frequency via a general linear ANOVA and via a negative binomial for apnea frequency. We subsequently obtained an autocorrelation function of each respiratory trace using a 10 s (5001 sample) window that encompassed at least 18 breaths that was devoid of spontaneous apneas and/or movement-related artifact.

3. Analysis

The ACF is the Pearson product-moment correlation of a signal with a copy of itself that is delayed in time. The delay is measured in lags, wherein each lag corresponds to a delay of a *single data point* – an estimate of where a given data point will occur (some) time later based on upon its current location. Representative ACFs for a saline-exposed pup are shown in Fig. 1. Each ACF highlights between-group differences in the regularity of the functions, peak heights and the rates at which the peak heights approach zero as a function of the elapsed time. By contrasting ACFs in this manner it is possible to make statements regarding the stability of a (given) measure for each rat pup over time (see below). Note that in applying the ACF to the respiratory trace directly, the ACF considers the stability of *individual data points* over successive breaths. It does not represent an average of data points across breaths as is the case in a Poincare plot. In this regard, the ACF can be used to quantify stability based on instantaneous samples of the digitized trace, affording a highly sensitive view of system stability over the short, mid-range or long term.

The application of the ACF to a data trace is demonstrated in Fig. 2, which shows a section of a representative respiratory trace obtained from a saline-exposed rat pup. The trace as shown in Panel A when overdrawn with a time lagged copy of itself (Panels B, C and D) can be used to assess instantaneous similarities and differences in chest wall motion as a function of time. The differences in respiratory patterning subsequently were assessed using repeated-measures ANOVA with one between-subjects factor,

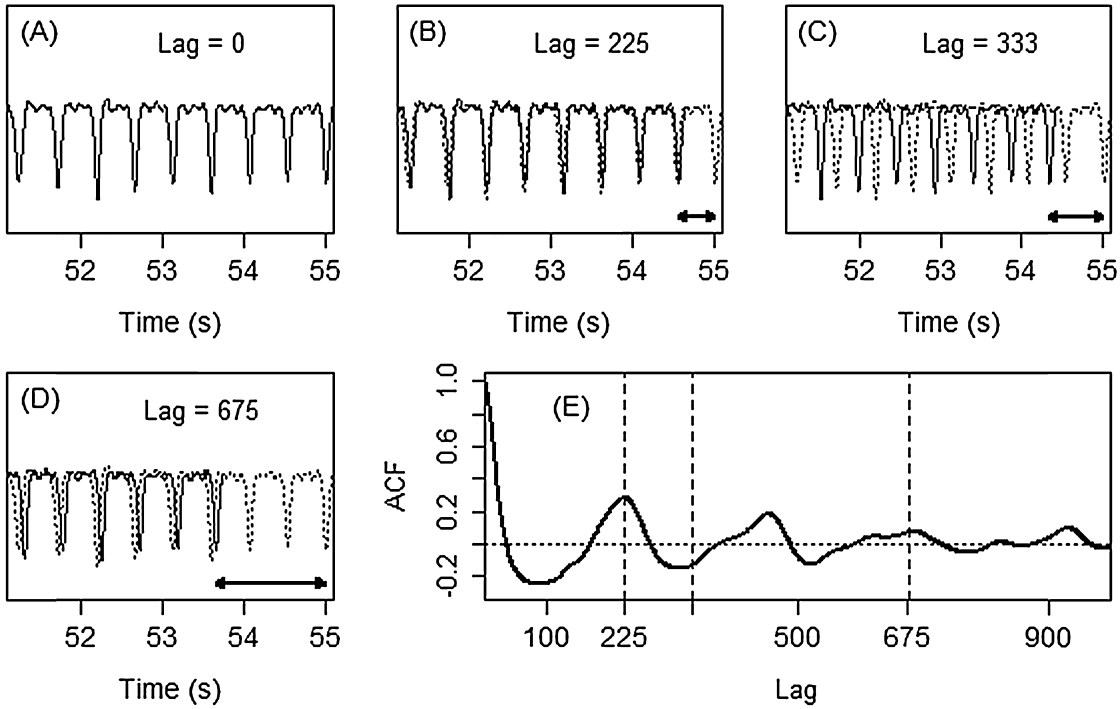

Fig. 2. (A–D) Representative chest wall traces (5.0 s) from a saline-exposed rat. Solid and dotted lines contrast the respiratory traces with a trace that is time shifted. The offset between the traces is the time lag and is indicated in each panel. Arrows in each panel indicate the magnitude of the lag in each case. Panels (B) and (D) are examples of lags equal to integer multiples of the period and panel (C) shows a shift of an incomplete number of cycles and demonstrate the potential to predict timing of events. Panel (E) shows the ACF of the entire recording with vertical lines indicating the ACF value associated with panels B–D.

experimental group, and one within-subjects factor, breath distance. Greenhouse–Geisser corrections for sphericity (Greenhouse and Geisser, 1959) were employed as appropriate.

4. Results

Consistent with previous literature, DNE had no effect on body mass relative to age-matched saline-treated pups ($p = 0.174$) (St-John and Leiter, 1999; Fewell et al., 2001; Robinson et al., 2002; Huang et al., 2004) and pups in both groups made steady gains in weight with post-natal age ($p < 0.001$). Pups of all ages exhibited spontaneous apneas however neither apnea frequency nor duration differed between DNE and saline treated pups and nor were they different as a function of post-natal age (data not shown). Averages for heart rate and breathing rate also failed to distinguish between the two groups ($p = 0.678$) (data not shown).

As shown in Fig. 2A, the respiratory trace is an almost periodic signal and the shape of each chest wall excursion is similar, but not identical, between cycles. The alignment of the two signals is more or less correlated depending upon the time-delay, and two signals attain maximal alignment at (some) fixed interval that is designated as the period (P) of the underlying function. Maximal alignment results in local maxima in the ACF (see for example Fig. 2E) for lag values that are near integer multiples of the period (and see Fig. 2B and D). By extension, low values occur at time points between peaks (see for example Fig. 2C). The time point associated with the ACF highest maximum value (i.e., at lag 225 in Fig. 2E) is the period of the function (P) (Boersma, 1993) and can be used to derive the average breathing rate for each record. And, since P is the period of a breath, the value of the ACF at integer multiples of P yields the correlation of the respiratory trace with itself some number of breaths away, based on the global estimate of average breath duration. Thus, the value of the ACF at P quantitates the similarity of a breath to the breath that follows (Fig. 2B), the value of the ACF at $2P$ relates a breath to the breath two cycles away, and the value of the ACF at nP gives information regarding a breath and the breath n cycles away. On this basis, the value of the ACF at each of these locations provides an estimate of respiratory stability as a function of *breath distance*.

A representative chest wall motion trace obtained from a nicotine-exposed pup is shown in Fig. 3. This trace has been subject to the same unpacking of the calculation of the ACF as presented in Fig. 2 and underscores several key differences between the nicotine and saline exposed pups. Note first that there is more breath to breath variability evident in the chest wall excursion trace in this DNE pup relative to a saline-exposed pup of the same age (compare Fig. 3A with Fig. 2A). A greater variability is reflected in a more irregular ACF shown in Fig. 3E (relative to Fig. 2E) and which serves as a direct indicator of system instability. Second, there is evident misalignment of the two signals in Fig. 3B, compared to a near perfect overlap of signals in the saline-exposed pup of the same age (see Fig. 2B). The misalignment results in a lower first-peak maximal value in Fig. 3E (relative to 2E), and indicates that over the course of a single respiratory cycle, the DNE rat pup begins to depart from respiratory regularity (Fig. 4). Indeed, the third ACF peak for the saline-exposed pup (Fig. 2E) has a value of ~0.2 that is equal to the value of the first peak in the ACF for the DNE pup (Fig. 3E). Whereas saline exposed pups exhibit comparable chest wall excursion patterns for instantaneous events one, two and three breath cycles removed from the first, the trajectory of chest wall excursion exhibited by DNE pups is highly dissimilar both in magnitude and timing such that there is remarkably little similarity between *consecutive breaths* (Fig. 3D). Thus, chest wall motions in DNE pups vary considerably within very short time windows whereas breath cycles of saline exposed pups exhibit minimal variation across multiple breath cycles (Fig. 2D).

Group distributions for ACF values as a function of *breath distance* are presented in Fig. 5A. This analysis reveals a main effect for breath distance [$F(3, 96) = 99.0$, $p < 0.0001$], a breath

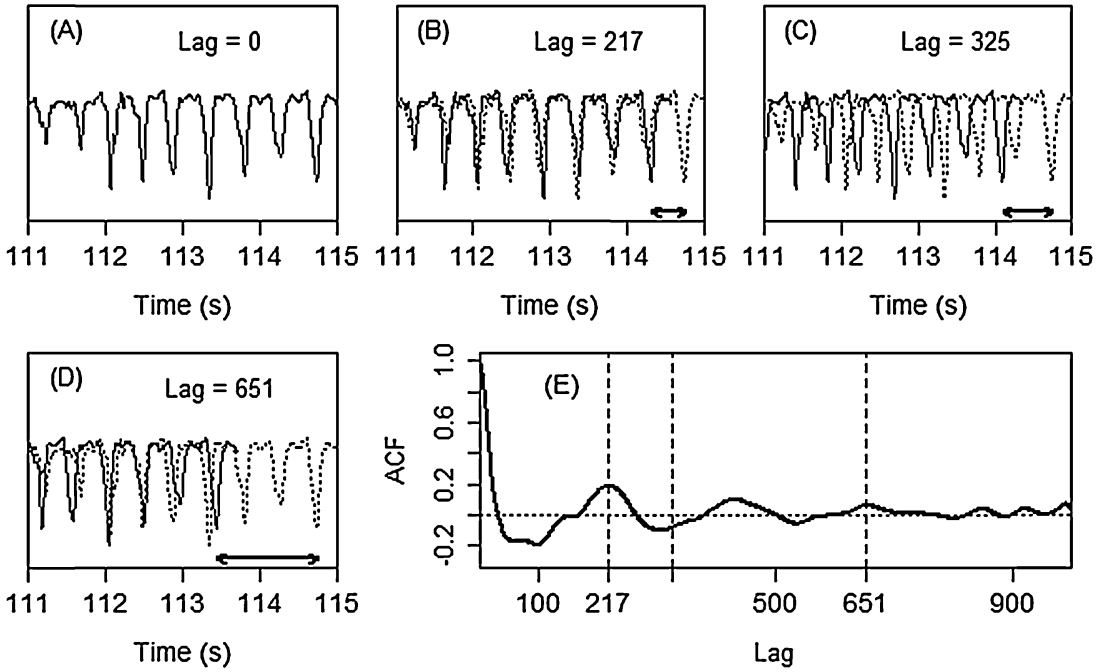

Fig. 3. (A–D) Sections (5 s) of a longer respiratory trace from a nicotine-exposed rat. (A–D) Solid and dotted lines contrast the respiratory traces with lagged versions of each trace. The offset between the traces, measured in lags, is indicated in each panel. Arrows indicate the magnitude of the shift in time in each panel. Panels (B) and (D) represent lags equal to integer multiples of the period, while panel (C) show a shift of an incomplete number of cycles. (E) The ACF of the entire record (not simply the 5 s window displayed here). Vertical lines indicate ACF values associated with panels B–D.

distance × treatment group interaction [$F(3, 96) = 4.05$, $p = 0.016$], and a main effect for treatment group [$F(1, 32) = 0.18$, $p = 0.67$]. The absence of a significant main effect for treatment group and the significant breath distance × treatment group interaction indicate discrepant effects as a function of time for the two groups. To assess group differences in the rates of decline of the ACF (indicated by the treatment × breath distance interaction), we determined the rate of decline of respiratory stability for each rat, as a function of the first three breaths. The distribution of these slopes is presented in Fig. 5B and highlights a difference between the groups ($p = 0.006$) and confirms markedly reduced respiratory stability in DNE pups relative to their saline-exposed peers.

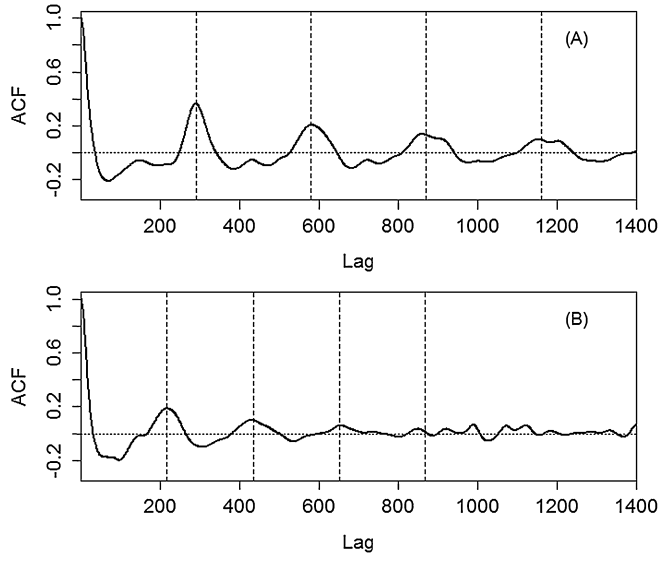

Fig. 4. Representative autocorrelation functions derived from respiratory traces obtained from two pups: (A) a saline-exposed pup and (B) a nicotine-exposed pup. Vertical lines indicate the expected locations of local maxima associated with contiguous breaths given the estimated breathing-rate for each record.

5. Discussion

The calculation of the ACF uses an arbitrary time window and can be performed online to obtain a visual summary of respiratory rate and stability for a given recording epoch. In this case, when the ACF was applied to chest wall traces it detected greater instability in DNE pups than for sham-treated pups. We consider this an important finding given that standard (i.e., averaged) analyses of breathing frequency, heart rate and apnea counts as applied here and elsewhere previously (Huang et al., 2004), failed to differentiate between the groups. Although saline and DNE pups attained the same measure of similarity within four breath cycles, the rate at which breaths departed from similarity differed for the two groups. Thus, multiple breaths taken by saline-exposed pups differ modestly from one another whereas single breaths taken by DNE pups are poor approximations of the preceding and following breaths, and reach a nadir in similarity within 3 breaths. The rapid decline in the ACF exhibited by DNE pups is evidence of significant respiratory instability that would otherwise pass undetected.

5.1. Critique of method

The effect of pre- or perinatal tobacco smoke or nicotine exposure in human neonates remains somewhat controversial due in part to a broad range of experimental protocols. Because of the heterogeneity of approaches and the inability to identify common results or mechanisms, even fundamental questions may better be addressed initially in (non-human) mammalian neonates (Stephan-Blanchard et al., 2013). In this case, we studied rat pups exposed either to saline (control) or to nicotine until post-natal day 10. Nicotine and saline infusion was achieved via osmotic minipump that delivers substrate on a controlled and continuous basis avoiding fluctuations in concentration and minimizing stress. In

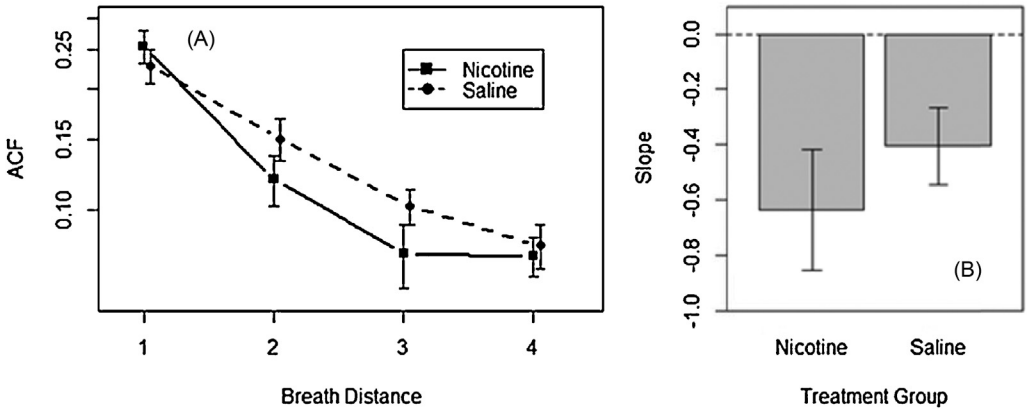

Fig. 5. (A) Distribution of ACF values across breath number and treatment group. Error bars indicate standard error of the mean. (B) Decline in the ACF as a function of successive breaths (i.e., breath distance) for DNE vs saline-exposed pups. Error bars indicate standard deviations.

this case, the dose rate was set at 6 mg kg^{-1} day^{-1} of nicotine bitartrate, equivalent to 2.1 mg kg^{-1} day^{-1} of free base nicotine and to the levels detected in moderate-heavy smokers (Benowitz et al., 2002) but does not exert any deleterious effects on fetal growth (Bamford et al., 1996). Although mini-pump delivery provides the opportunity to isolate nicotine from the confounding effect of tobacco smoke, pump delivery also ensures stable nicotine concentrations that cannot replicate the large, transient fluctuations in nicotine concentration experienced by the human embryo of a mother that smokes (McKinney et al., 2010; Rose et al., 1999).

We elected to study pups on P7–10 to approximate the perinatal period (Adlard et al., 1973; Clancy et al., 2007; Dobbing and Sands, 1979; Romijn et al., 1991). This age range encompasses both preterm and very early post-natal periods of the human infant. Although the risk for respiratory instability and SIDS is predicted to peak at P12–13, corresponding to the "critical period" in rat brainstem development (Liu et al., 2006; Liu and Wong-Riley, 2010; Wong-Riley and Liu, 2008), the present findings serve as proof of concept and demonstrate the potential to apply ACF in detection of respiratory disturbances at the very earliest development stages.

The technique for tracking chest wall excursions in pups of this size (i.e., <30 g) has been reported previously, and faithfully tracks chest wall excursions during rest breathing when pups are quiet (Kidder et al., 2014). To reduce the potential for movement related artifact, we sedated pups and selected Inactin for this purpose based on duration of action and minimal alteration of physiological functions in rats (Lorenz, 2002; Walter et al., 1989). We took care to titrate sedation on the basis of breathing frequency, which did not drop below 110 ± 10 breaths min^{-1} from a baseline of 170 ± 10 breaths min^{-1}. Although barbiturates enhance gamma-aminobutyric acid mediated chloride currents (30), the primary inhibitory signal within the CNS, because pups *in both DNE and saline groups* were exposed to the same sedation protocol we consider this manipulation an experimental constant. Consistent with mild sedation, pups in both groups exhibited comparable responsiveness to mild hypoxia ($F_IO_2 = 0.14$) and became mobile within ~2.0 min of exposure, confirming preservation of arousal responses (Romijn et al., 1991). Note that due to pup mobility in mild hypoxia, we were unable to obtain measures of respiratory stability from either group in this condition.

5.2. Respiratory stability

Previous in vitro studies have shown that DNE affects synaptic mechanisms and chemosensory properties of the respiratory network (Eugenin et al., 2008; Fregosi and Pilarski, 2008). Moreover, fictive respiratory cycles recorded in DNE brainstem preparations are more irregular than those observed in control animals (Eugenin et al., 2008). It is worth remembering however, that respiratory dysfunctions in vivo are relatively rare-events (Campos et al., 2009) and the majority of infants born to mothers that smoke *will not* succumb to SIDS. Somewhat surprisingly, for those infants who do fall victim to SIDS, there is very little evidence of gross respiratory abnormality (Bamford and Carroll, 1999), although subtle abnormalities in breath-to-breath interval variability have been reported (Schechtman et al., 1996).

Identifying factors that mitigate or augment respiratory instablity remains a major clinical challenge. In this case, it was necessary to sedate pups to minimize movement artifact but whether temporary sedation for surgery or pain management serves to mitigate or further impair the progression toward and devlopment of long term respiratory stability warrants investigation (McPherson and Grunau, 2014). Certainly, the application of ACFs in these more clinical contexts may make it possible to determine the rate at which a data point/s at one time in a breath cycle depart from the normal trajectory at the same time in subsequent breaths. The approach is highly sensitive to any abberation in central and/or peripheral mechanisms of respiratory control. Thus, given some perturbation (e.g., lowered blood oxygen level, lowered temperature) the initial ventilatory response will decay gradually resulting in higher local maxima in the ACF that reflect greater similarity and thus stability estimates. However, if regulatory mechansisms (e.g., chemoreceptor, mechanoreceptor, or homeostatic) exhibit a heightened sensitivity then any modest perturbation, whether in blood gases, body temperature or state may exacerbate the respiratory adjustment resulting in overshoot drive responses and lower local ACF maxima that reflect greater instability (Szlyk and Jennings, 1987).

5.3. Summary

Despite evidence that DNE affects development of central respiratory control and increases the risk for central and obstructive apneas (Golding, 1997; Kahn et al., 1994), the signs or symptoms of significant respiratory impairment are very often too subtle to detect. Accordingly, our focus was on the potential to distinguish between DNE and saline exposed rat pups using a global index of respiratory system stability that compares instantaneous data points within and across breath cycles. Although chest wall motions are used extensively in clinical research and pulmonary function testing, they are not as well utilized at the bedside. In view of the present findings obtained in rat pups, we suggest that the ACF might next be applied to respiratory motion traces obtained from human infants and available to clinicians via commercially

available patient monitoring systems. Because the ACF is applied to time series data and does not rely upon traditional respiratory averages (i.e., inspiratory/expiratory time, tidal volume or breathing frequency) or summary statistics it offers a highly sensitive means of detecting instability (Tobin et al., 1995) that requires minimal signal processing and can assess multiple dimensions of each breath simultaneously.

Contributions

Conception and design of the experiments – Santiago Barreda, Ian J. Kidder and E. Fiona Bailey. Collection, analysis and interpretation of data – Santiago Barreda, Ian J. Kidder, Jordan A. Mudery and E. Fiona Bailey. Drafting the article or revising it critically for important intellectual content – Santiago Barreda and E. Fiona Bailey.

References

Adlard, B.P., Dobbing, J., Smart, J.L., 1973. An alternative animal model for the full-term small-for-dates human baby. Biol. Neonate 23, 95–108.

Bamford, O.S., Carroll, J.L., 1999. Dynamic ventilatory responses in rats: normal development and effects of prenatal nicotine exposure. Respir. Physiol. 117, 29–40.

Bamford, O.S., Schuen, J.N., Carroll, J.L., 1996. Effect of nicotine exposure on postnatal ventilatory responses to hypoxia and hypercapnia. Respir. Physiol. 106, 1–11.

Barrett, K.T., Kinney, H.C., Li, A., Daubenspeck, J.A., Leiter, J.C., Nattie, E.E., 2012. Subtle alterations in breathing and heart rate control in the 5-HT1A receptor knockout mouse in early postnatal development. J. Appl. Physiol. 113, 1585–1593.

Benowitz, N.L., Hansson, A., Jacob 3rd, P., 2002. Cardiovascular effects of nasal and transdermal nicotine and cigarette smoking. Hypertension 39, 1107–1112.

Boersma, P., 1993. Accurate short-term analysis of the fundamental frequency and the harmonics to noise ration of a sampled sound. Proc. Inst. Phon. Sci. 17, 97–110.

Brennan, M., Palaniswami, M., Kamen, P., 2002. Poincare plot interpretation using a physiological model of HRV based on a network of oscillators. Am. J. Physiol. Heart Circ. Physiol. 283, H1873–H1886.

Campos, M., Bravo, E., Eugenin, J., 2009. Respiratory dysfunctions induced by prenatal nicotine exposure. Clin. Exp. Pharmacol. Physiol. 36, 1205–1217.

Clancy, B., Finlay, B.L., Darlington, R.B., Anand, K.J., 2007. Extrapolating brain development from experimental species to humans. Neurotoxicology 28, 931–937.

Cohen, G., Roux, J.C., Grailhe, R., Malcolm, G., Changeux, J.P., Lagercrantz, H., 2005. Perinatal exposure to nicotine causes deficits associated with a loss of nicotinic receptor function. Proc. Natl. Acad. Sci. USA 102, 3817–3821.

Dick, T.E., Mims, J.R., Hsieh, Y.H., Morris, K.F., Wehrwein, E.A., 2014. Increased cardiorespiratory coupling evoked by slow deep breathing can persist in normal humans. Respir. Physiol. Neurobiol.

Dobbing, J., Sands, J., 1979. Comparative aspects of the brain growth spurt. Early Hum. Dev. 3, 79–83.

Duncan, J.R., Randall, L.L., Belliveau, R.A., Trachtenberg, F.L., Randall, B., Habbe, D., Mandell, F., Welty, T.K., Iyasu, S., Kinney, H.C., 2008. The effect of maternal smoking and drinking during pregnancy upon (3)H-nicotine receptor brainstem binding in infants dying of the sudden infant death syndrome: initial observations in a high risk population. Brain Pathol. 18, 21–31.

Eugenin, J., Otarola, M., Bravo, E., Coddou, C., Cerpa, V., Reyes-Parada, M., Llona, I., von Bernhardi, R., 2008. Prenatal to early postnatal nicotine exposure impairs central chemoreception and modifies breathing pattern in mouse neonates: a probable link to sudden infant death syndrome. J. Neurosci. 28, 13907–13917.

Fewell, J.E., Smith, F.G., Ng, V.K., 2001. Prenatal exposure to nicotine impairs protective responses of rat pups to hypoxia in an age-dependent manner. Respir. Physiol. 127, 61–73.

Fregosi, R.F., Pilarski, J.Q., 2008. Prenatal nicotine exposure and development of nicotinic and fast amino acid-mediated neurotransmission in the control of breathing. Respir. Physiol. Neurobiol. 164, 80–86.

Golding, J., 1997. Sudden infant death syndrome and parental smoking – a literature review. Paediatr. Perinatal. Epidemiol. 11, 67–77.

Greenhouse, S.W., Geisser, S., 1959. On methods in the analysis of profile data. Psychometrics 24, 95–112.

Hilaire, G., Voituron, N., Menuet, C., Ichiyama, R.M., Subramanian, H.H., Dutschmann, M., 2010. The role of serotonin in respiratory function and dysfunction. Respir. Physiol. Neurobiol. 174, 76–88.

Huang, Y.H., Brown, A.R., Costy-Bennett, S., Luo, Z., Fregosi, R.F., 2004. Influence of prenatal nicotine exposure on postnatal development of breathing pattern. Respir. Physiol. Neurobiol. 143, 1–8.

Jaiswal, S.J., Pilarski, J.Q., Harrison, C.M., Fregosi, R.F., 2013. Developmental nicotine exposure alters AMPA neurotransmission in the hypoglossal motor nucleus and pre-Botzinger complex of neonatal rats. J. Neurosci. 33, 2616–2625.

Kahn, A., Groswasser, J., Sottiaux, M., Kelmanson, I., Rebuffat, E., Franco, P., Dramaix, M., Wayenberg, J.L., 1994. Prenatal exposure to cigarettes in infants with obstructive sleep apneas. Pediatrics 93, 778–783.

Kidder, I.J., Mudery, J.A., Bailey, E.F., 2014. Neural drive to respiratory muscles in the spontaneously breathing rat pup. Respir. Physiol. Neurobiol. 202, 64–70.

Liu, Q., Lowry, T.F., Wong-Riley, M.T., 2006. Postnatal changes in ventilation during normoxia and acute hypoxia in the rat: implication for a sensitive period. J. Physiol. 577, 957–970.

Liu, Q., Wong-Riley, M.T., 2010. Postnatal changes in the expressions of serotonin 1A, 1B, and 2A receptors in ten brain stem nuclei of the rat: implication for a sensitive period. Neuroscience 165, 61–78.

Lorenz, J.N., 2002. A practical guide to evaluating cardiovascular, renal, and pulmonary function in mice. Am. J. Physiol. Regul. Integr. Comp. Physiol. 282, R1565–R1582.

Luo, Z., Costy-Bennett, S., Fregosi, R.F., 2004. Prenatal nicotine exposure increases the strength of GABA(A) receptor-mediated inhibition of respiratory rhythm in neonatal rats. J. Physiol. 561, 387–393.

Machaalani, R., Say, M., Waters, K.A., 2011. Effects of cigarette smoke exposure on nicotinic acetylcholine receptor subunits alpha7 and beta2 in the sudden infant death syndrome (SIDS) brainstem. Toxicol. Appl. Pharmacol. 257, 396–404.

Machaalani, R., Waters, K.A., 2008. Neuronal cell death in the sudden infant death syndrome brainstem and associations with risk factors. Brain 131, 218–228.

McKinney, D.L., Davies, B.D., Gogova, M., Adams, W.M., Lewis, W., Powell, C., Iyer, S.S., Garnett, W.R., Karnes, H.T., Kobal, G., Barr, W.H., 2010. Rapid automated blood sampling system for pharmacokinetics studies of cigarette smoking. Nicotine Tob. Res. 12, 319–325.

McPherson, C., Grunau, R.E., 2014. Neonatal pain control and neurologic effects of anesthetics and sedatives in preterm infants. Clin. Perinatol. 41, 209–227.

Mitchell, E.A., Milerad, J., 2006. Smoking and the sudden infant death syndrome. Rev. Environ. Health 21, 81–103.

Robinson, D.M., Peebles, K.C., Kwok, H., Adams, B.M., Clarke, L.L., Woollard, G.A., Funk, G.D., 2002. Prenatal nicotine exposure increases apnoea and reduces nicotinic potentiation of hypoglossal inspiratory output in mice. J. Physiol. 538, 957–973.

Romijn, H.J., Hofman, M.A., Gramsbergen, A., 1991. At what age is the developing cerebral cortex of the rat comparable to that of the full-term newborn human baby? Early Hum. Dev. 26, 61–67.

Rose, J.E., Behm, F.M., Westman, E.C., Coleman, R.E., 1999. Arterial nicotine kinetics during cigarette smoking and intravenous nicotine administration: implications for addiction. Drug Alcohol Depend. 56, 99–107.

Schechtman, V.L., Lee, M.Y., Wilson, A.J., Harper, R.M., 1996. Dynamics of respiratory patterning in normal infants and infants who subsequently died of the sudden infant death syndrome. Pediatr. Res. 40, 571–577.

Serra, A., Brozoski, D., Hedin, N., Franciosi, R., Forster, H.V., 2001. Mortality after carotid body denervation in rats. J. Appl. Physiol. 91, 1298–1306.

Slotkin, T.A., Cho, H., Whitmore, W.L., 1987. Effects of prenatal nicotine exposure on neuronal development: selective actions on central and peripheral catecholaminergic pathways. Brain Res. Bull. 18, 601–611.

Smith, A.M., Dwoskin, L.P., Pauly, J.R., 2010. Early exposure to nicotine during critical periods of brain development: mechanisms and consequences. J. Pediatr. Biochem. 1, 125–141.

St-John, W.M., Leiter, J.C., 1999. Maternal nicotine depresses eupneic ventilation of neonatal rats. Neurosci. Lett. 267, 206–208.

Stephan-Blanchard, E., Bach, V., Telliez, F., Chardon, K., 2013. Perinatal nicotine/smoking exposure and carotid chemoreceptors during development. Respir. Physiol. Neurobiol. 185, 110–119.

Szlyk, P.C., Jennings, D.B., 1987. Effects of hypercapnia on variability of normal respiratory behavior in awake cats. Am J Physiol. 252 (3), R538–R547.

Tobin, M.J., Yang, K.L., Jubran, A., Lodato, R.F., 1995. Interrelationship of breath components in neighboring breaths of normal eupneic subjects. Am. J. Respir. Crit. Care Med. 152, 1967–1976.

Walter, S.J., Zewde, T., Shirley, D.G., 1989. The effect of anaesthesia and standard clearance procedures on renal function in the rat. Q. J. Exp. Physiol. 74, 805–812.

Waters, K.A., Meehan, B., Huang, J.Q., Gravel, R.A., Michaud, J., Cote, A., 1999. Neuronal apoptosis in sudden infant death syndrome. Pediatr. Res. 45, 166–172.

Willinger, M., James, L.S., Catz, C., 1991. Defining the sudden infant death syndrome (SIDS): deliberations of an expert panel convened by the National Institute of Child Health and Human Development. Pediatric pathology/affiliated with the International Paediatric Pathology Association, vol. 11., pp. 677–684.

Wong-Riley, M.T., Liu, Q., 2008. Neurochemical and physiological correlates of a critical period of respiratory development in the rat. Respir. Physiol. Neurobiol. 164, 28–37.